Effect of pulse-shape uncertainty on the accuracy of deconvolved lidar profiles

T. N. Dreischuh, L. L. Gurdev, and D. V. Stoyanov

Institute of Electronics, Bulgarian Academy of Sciences, 72 Tzarigradsko Shosse Boulevard, 1784 Sofia, Bulgaria

Received February 7, 1994; revised manuscript received August 8, 1994; accepted August 9, 1994

The effect of random and deterministic pulse-shape uncertainties on the accuracy of the Fourier deconvolution algorithm for improving the resolution of long-pulse lidars is investigated theoretically and by computer simulations. Various cases of pulse uncertainties are considered including those that are typical of Doppler lidars. It is shown that the retrieval error is a consequence of two main effects. The first effect consists of a shift up or down (depending on the sign of the uncertainty integral area) of the lidar profile as a whole, proportionally to the ratio of the pulse uncertainty area to the true pulse area. The second effect consists of additional amplitude and phase distortions of the spectrum of the small-scale inhomogeneities of the lidar profile. The results obtained allow us to predict the order and the character of the possible distortions and to choose ways to reduce or prevent them.

1. INTRODUCTION

The lidar systems that use long sensing laser pulses (e.g., emitted by a TE (TEA) CO_2 laser[1,2] have low spatial resolution that is of the order of the pulse length if the integration period of the photodetector is negligible. In this case the lidar return signal $F(t)$ at moment t after the pulse emission is described by the convolution[3]

$$F(t) = \int_{-\infty}^{\infty} S(t - 2z'/c)\Phi(z')\mathrm{d}z' \qquad (1)$$

of the pulse shape $S(\vartheta)$ and the maximum-resolved (obtainable by a sufficiently short laser pulse) lidar profile $\Phi(z)$. In Eq. (1), c is the speed of light, z' is the coordinate along the line of sight, $S(\vartheta) = \mathcal{P}(\vartheta)/\mathcal{P}_p$, $\mathcal{P}(\vartheta)$ is the pulse power shape and $\mathcal{P}_p$ is its peak value, and ϑ is a time variable. As a result of the convolution effect in the case of CO_2 Doppler lidars that is mentioned in Refs. 4 and 5, important information about the small-scale variations of the backscattering within the long-resolution cell (typically 200–500 m) is lost during the Doppler velocity measurements. This loss of information expresses the well-known conflict between the range and the velocity resolutions in Doppler radars and lidars. An approach for retrieval of the mean atmospheric backscattering coefficient and its fluctuations has been developed in Refs. 6 and 7 for CO_2 differential absorption lidar measurements. This approach is based on the so-called correction function and requires some preliminary information (provided by the differential absorption lidar technique) about the atmospheric absorption and about the relation between the absorption and the scattering.

A direct way to improve the lidar resolution is to solve Eq. (1) with respect to $\Phi(z)$. That is why earlier we developed[8,9] deconvolution techniques to invert Eq. (1) when the pulse shape is known without any uncertainty. These techniques are based on Fourier transformation, the Volterra integral equation, or a recurrence relation and ensure good quality in the retrieval of the fine structure of the backscattering inhomogeneities. Such an approach is essential for single-wavelength Doppler lidars. It does not require preliminary information about the absorption or about the spatial spectra of the inhomogeneities. As a result, the range resolution of the backscattering profiles becomes better than that of the velocity profiles. The application of the deconvolution techniques to Doppler lidar data from the National Oceanic and Atmospheric Administration was demonstrated in Refs. 10 and 11, in which some of the statistical characteristics of the data within the Doppler resolution cell had been determined.

As briefly noted in Refs. 8 and 12, because of various factors the shape $S(\vartheta)$ might be determined with some regular (deterministic) or random uncertainties that lead to errors in the determination of $\Phi(z)$. As an example, the spike in the laser pulse shape of TEA CO_2 Doppler lidars is often not well recorded; i.e., it is cut, in the output raw data.[13] The purpose of the present study, being in a sense an addition to that of Ref. 8, is to investigate the relations between the pulse-shape uncertainties and the corresponding errors in the restoration of the lidar profiles $\Phi(z)$. This problem is of importance for the analysis of the limitations of the deconvolution techniques as well as for the analysis of the requirements that are satisfied by the lidar data recorders.

2. PULSE-UNCERTAINTY INFLUENCE ON THE ACCURACY OF THE DECONVOLVED LIDAR PROFILES

The Fourier deconvolution algorithm is based on the expression[8]

$$\Phi(z \equiv ct/2) = (\pi c)^{-1} \int_{-\infty}^{\infty} [\tilde{F}(\omega)/\tilde{S}(\omega)]\exp(-j\omega t)\mathrm{d}\omega\,, \qquad (2)$$

where $\tilde{S}(\omega) = \int_{-\infty}^{\infty} S(t')\exp(j\omega t')\mathrm{d}t'$ and $\tilde{F}(\omega) = \int_{-\infty}^{\infty} F(t')\exp(j\omega t')\mathrm{d}t'$ are Fourier transforms of S and F, respectively; j is imaginary unity; and $\tilde{\Phi}(\omega) \equiv \tilde{\Phi}(2\omega/c) = \tilde{F}(\omega)/\tilde{S}(\omega) = (c/2)\int_{-\infty}^{\infty} \Phi(z' = ct'/2)\exp(j\omega t')\mathrm{d}t'$. Let

0740-3232/95/020301-06$06.00

us represent the measured pulse shape $S_m(\vartheta)$ as a sum $S_m(\vartheta) = S(\vartheta) + f(\vartheta)$ of the true pulse shape $S(\vartheta)$ and a deterministic or random uncertainty $f(\vartheta)$ in its measurement. Then the Fourier deconvolution error is obtained on the basis of Eq. (2) as

$$\begin{aligned}\delta_\Phi(z = ct/2) &= \Phi_r(z) - \Phi(z) \\ &= -(\pi c)^{-1}\int_{-\infty}^{\infty}\tilde{\Phi}(\omega)\tilde{f}(\omega)[\tilde{S}(\omega) + \tilde{f}(\omega)]^{-1} \\ &\quad \times \exp(-j\omega t)\mathrm{d}\omega\,, \end{aligned} \tag{3}$$

where $\Phi_r(z)$ is the lidar profile restored with use of the measured pulse shape $S_m(\vartheta)$ and $\tilde{f}(\omega) = \int_{-\infty}^{\infty} f(\vartheta)\exp(j\omega\vartheta)\mathrm{d}\vartheta$ is the Fourier transform of $f(\vartheta)$. As far as $\tilde{\Phi}(\omega)$, $\tilde{S}(\omega)$, and $\tilde{f}(\omega)$ are expressible as integrals over all values of a spatial variable $z' = ct'/2$, Eq. (3) does not represent, in general, a local dependence of $\delta_\Phi(z)$ on $\Phi(z)$ and $f(z)$.

The Fourier transformation of Eq. (3) leads to the relation $\tilde{\delta}_\Phi(\omega)\tilde{S}_m(\omega) = -(2/c)\tilde{\Phi}(\omega)\tilde{f}(\omega)$, where $\tilde{S}_m(\omega) = \tilde{S}(\omega) + \tilde{f}(\omega)$, and $\tilde{\delta}_\Phi(\omega) = \int_{-\infty}^{\infty}\delta_\Phi(z = ct/2)\exp(j\omega t)\mathrm{d}t$ are the Fourier transforms of $S_m(\vartheta)$ and $\delta_\Phi(z = ct/2)$, respectively. The inverse Fourier transform of the last relation leads to the equation

$$S_m * \delta_\Phi = -f * \Phi\,, \tag{4}$$

which expresses the nonlocal interconnection between the uncertainty f and the error δ_Φ ($*$ denotes a convolution). The sense of Eq. (4) is that, for instance, a positive-sign uncertainty $f(\vartheta) > 0$ is equivalent to a pseudocontribution to the integration in Eq. (1) [to the signal $F(t)$]. Correspondingly, the deconvolution process compensates this pseudocontribution by lowering the restored profile Φ_r with respect to Φ.

A. Deterministic Uncertainties

Here we analyze some general features of the influence of different types of deterministic uncertainty on the retrieval accuracy. Let us first consider $f(\vartheta)$ as a slowly varying [in comparison with $S(\vartheta)$] prolonged deterministic function of ϑ with constant sign and assume that $f(\vartheta) \ll S(\vartheta)$. Correspondingly, the spectrum $\tilde{f}(\omega)$ will be narrow compared with $\tilde{S}(\omega)$ and will be concentrated around $\omega = 0$. Then we may neglect $\tilde{f}(\omega)$ in the integrand denominator of Eq. (3) and integrate over ω, considering $\tilde{S}(\omega)$ to be a constant equal to $\tilde{S}(0) = \int_{-\infty}^{\infty} S(\vartheta)\mathrm{d}\vartheta = \tau_{\mathrm{eff}}$, which may be interpreted as the effective pulse duration. In this way, from Eq. (3) we obtain the following expression for δ_Φ:

$$\begin{aligned}\delta_\Phi(z = ct/2) &\approx -{p_{\mathrm{eff}}}^{-1}\int_{-\infty}^{\infty}\Phi(z')f(t - 2z'/c)\mathrm{d}z' \\ &= -(p_{\mathrm{un}}/p_{\mathrm{eff}})\overline{\Phi}(t)\,. \end{aligned} \tag{5}$$

Relation (5) shows that the error δ_Φ is proportional to the magnitudes of Φ and f and involves interactions of f with all values of Φ within the spatial interval of the uncertainty. In relation (5), $p_{\mathrm{eff}} = (c/2)\tau_{\mathrm{eff}}$, $p_{\mathrm{un}} = (c/2)\int_0^{\infty} f(\vartheta)\mathrm{d}\vartheta$, and the value of $\overline{\Phi} = {p_{\mathrm{un}}}^{-1}(f * \Phi)$ may be interpreted as being weighted by the uncertainty average of Φ. Here p_{eff} and p_{un} may be considered to be some effective pulse and uncertainty areas, respectively. In general, the uncertainty area p_{un} is an integral characteristic of the uncertainty effect. It may be positive or negative or even equal to zero for uncertainties with alternating signs.

A typical case of a fast-varying short-range uncertainty is the cut of a pulse spike. This case is essential for the CO_2 Doppler lidars. Here we may consider the pulse shape as a sum $S(\vartheta) = f_S(\vartheta) + f_R(\vartheta)$ of the spike $f_S(\vartheta)$ and the remaining tail $f_R(\vartheta)$. Thus $S_m(\vartheta) = f_R(\vartheta)$ and $f(\vartheta) = -f_S(\vartheta)$ so that Eq. (4) acquires the form $f_S * \Phi = f_R * \delta_\Phi$ from which, taking into account that $f_S * \Phi \approx p_S\Phi$, one may write

$$\overline{\delta_\Phi}(t)/\Phi(t) \approx p_S/p_R\,. \tag{6}$$

In relation (6), $p_S = (c/2)\int_0^{\infty} f_S(\vartheta)\mathrm{d}\vartheta$ is the effective spike area, $p_R = (c/2)\int_0^{\infty} f_R(\vartheta)\mathrm{d}\vartheta$ is the effective remainder area, and $\overline{\delta_\Phi}(t) = {p_R}^{-1}(f_R * \delta_\Phi)$ may be interpreted as a weighted, by the remainder, average of δ_Φ. It can be seen that the weighted error $\overline{\delta_\Phi} > 0$ and that the relative weighted error $\overline{\delta_\Phi}/\Phi$ is a positive constant approximately equal to p_S/p_R. This positive tendency suggests that a spike cut causes an elevation proportional to p_S/p_R of Φ_r as a whole with respect to Φ. Such an effect can be expected because the spike cut is a negative-sign uncertainty $f(\vartheta) = -f_S(\vartheta)$.

For a more detailed analysis of the spike-cut influence on the retrieval accuracy, we may consider the profile $\Phi(t)$ to be a sum $\Phi(t) = \Phi_{\mathrm{sm}}(t) + \Phi_v(t)$ of a smooth component $\Phi_{\mathrm{sm}}(t)$ and a fast-varying component $\Phi_v(t)$ describing the small-scale inhomogeneities of $\Phi(t)$. The mechanism of the uncertainty effect on the retrieval accuracy can be understood by analysis of the error in the restoration of the smooth component $\Phi_{\mathrm{sm}}(t)$ and in one of the harmonic (sine, cosine) components $\Phi_0(t)$ of the spectrum of the small-scale inhomogeneities. Then Eq. (3) acquires the form

$$\delta_\Phi(z = ct/2) = -(\pi c)^{-1}(J_1 + J_2)\,, \tag{7a}$$

where

$$J_1 = \int_{-\infty}^{\infty}\tilde{\Phi}_{\mathrm{sm}}(\omega)\mathcal{F}(\omega)\exp(-j\omega t)\mathrm{d}\omega\,, \tag{7b}$$

$$J_2 = \int_{-\infty}^{\infty}\tilde{\Phi}_0(\omega)\mathcal{F}(\omega)\exp(-j\omega t)\mathrm{d}\omega\,, \tag{7c}$$

and $\mathcal{F}(\omega) = \tilde{f}(\omega)[\tilde{S}(\omega) + \tilde{f}(\omega)]^{-1}$. $\tilde{\Phi}_{\mathrm{sm}}(\omega) = \int_{-\infty}^{\infty}\Phi_{\mathrm{sm}}(t)\exp(j\omega t)\mathrm{d}t$ and $\tilde{\Phi}_0(\omega) = \int_{-\infty}^{\infty}\Phi_0(t)\exp(j\omega t)\mathrm{d}t$ are the Fourier transforms of $\Phi_{\mathrm{sm}}(t)$ and $\Phi_0(t)$, respectively. For a spike cut we have $\tilde{f}(\omega) = -\tilde{f}_S(\omega) = -\int_{-\infty}^{\infty} f_S(\vartheta)\exp(j\omega\vartheta)\mathrm{d}\vartheta$ and $\tilde{S}(\omega) + \tilde{f}(\omega) = \tilde{f}_R(\omega) = \int_{-\infty}^{\infty} f_R(\vartheta)\exp(j\omega\vartheta)\mathrm{d}\vartheta$. Since a spike is short compared with $\Phi_{\mathrm{sm}}(t)$ and $\Phi_0(t)$, its spectral width $\Delta\omega$ exceeds the spectral widths $\Delta\omega_{\mathrm{sm}}$ and $\Delta\omega_0$ of $\tilde{\Phi}_{\mathrm{sm}}(\omega)$ and $\tilde{\Phi}_0(\omega)$. The spectral width $\Delta\omega_R$ of $\tilde{f}_R(\omega)$ satisfies the inequality $\Delta\omega \gg \Delta\omega_R \gg (\Delta\omega_{\mathrm{sm}}, \Delta\omega_0)$ because the pulse remainder $f_R(t)$ is shorter than $\Phi(t)$ and $\Phi_0(t)$ but is longer than $f_S(t)$. If the spike is shorter than the oscillation period $T_0 = 2\pi/\omega_0$ of $\Phi_0(t)$ so that $\Delta\omega > \omega_0$, the integration in J_1 is restricted by the profile of $\tilde{\Phi}_{\mathrm{sm}}(\omega)$ and is concentrated around $\omega = 0$, where $\tilde{f}(\omega) = -\tilde{f}_S(\omega) \approx -\tilde{f}_S(0)$

and $\tilde{S}(\omega) + \tilde{f}(\omega) = \tilde{f}_R(\omega) \approx \tilde{f}_R(0)$. Similarly, the integration in J_2 is concentrated around the peak frequencies $\omega = \pm\omega_0$ of $\tilde{\Phi}_0(\omega)$, where $\tilde{f}(\omega) \approx -\tilde{f}_S(0)$ and $\tilde{S}(\omega) + \tilde{f}(\omega) \approx \tilde{f}_R(\pm\omega_0)$. Then by using Eqs. (7b) and (7c) we obtain that

$$J_1 = -\pi c(\, p_S/p_R)\Phi_{\mathrm{sm}}(z = ct/2)\,, \tag{8a}$$

$$J_2 = -\pi c[\, p_S/p_R(\omega_0)]\{\cos[\varphi_R(\omega_0)]\Phi_0(z = ct/2) + 2\,\sin[\varphi_R(\omega_0)](\pi c)^{-1}\,\mathrm{Im}[J_a(z = ct/2)]\}, \tag{8b}$$

where $p_R(\omega) = (c/2)|\tilde{f}_R(\omega)|$ and $\varphi_R(\omega) = \arg[\tilde{f}_R(\omega)]$. The symbols $|\cdot|$ and $\arg[\cdot]$ denote the module and the argument, respectively, of a complex quantity. The quantity $J_a(t) = \int_0^\infty \Phi_0(\omega)\exp(-j\omega t)\mathrm{d}\omega$ is the analytical signal of $(\pi c)\Phi_0(t)$, and its imaginary part $\mathrm{Im}[J_a]$ is connected to its real part $\mathrm{Re}[J_a] = (\pi c/2)\Phi_0(t)$ by the Hilbert transformation. That is, $\mathrm{Im}[J_a(t)] = \pi^{-1}P\int_{-\infty}^{\infty}\{\mathrm{Re}[J_a(t')]/(t - t')\}\mathrm{d}t' = (c/2)P\int_{-\infty}^{\infty}[\Phi_0(t')/(t - t')]\mathrm{d}t'$, where P denotes the principal value of the integral at the singular point $t' = t$. Thus for a sine function $\Phi_0(t) = A_0\sin(\omega_0 t)$ (A_0 is the dimensional amplitude) we obtain that $\mathrm{Im}[J_a(t)] = -(\pi c/2)A_0\cos(\omega_0 t)$. For a cosine function $\Phi_0(t) = A_0\cos(\omega_0 t)$ we obtain $\mathrm{Im}[J_a(t)] = (\pi c/2)A_0\sin(\omega_0 t)$. In both cases, on the basis of Eqs. (7a), (8a), and (8b) we obtain the following estimate of the error caused by a spike cut:

$$\delta_\Phi(z = ct/2) \approx (\, p_S/p_R)\Phi_{\mathrm{sm}}(z = ct/2) + [\, p_S/p_R(\omega_0)]\Phi_0[z - z_{\mathrm{sh}}(\omega_0)], \tag{9}$$

where $z_{\mathrm{sh}}(\omega) = c\varphi_R(\omega)/(2\omega)$ is a spatial phase shift of the error oscillations with respect to the oscillations of Φ_0. The first term on the right-hand side of relation (9) describes an elevation of the smooth component $\Phi_{\mathrm{sm}}(z)$ proportional to p_S/p_R that leads to an elevation of Φ_r as a whole with respect to Φ. The second term describes both an increase in the amplitude of the oscillatory component $\Phi_0(z = ct/2)$ proportional to $p_S/p_R(\omega_0)$ and a phase shift $z_{\mathrm{sh}}(\omega_0)$ of its oscillations. It can be seen that these two effects are frequency dependent. It means that the spike cut leads to distortion of the spectrum of the inhomogeneities of the restored lidar profile in comparison with the spectrum of the original profile. The frequency dependence of the second term on the right-hand side of relation (9) is determined only by the spectrum $\tilde{f}_R(\omega)$ of the remainder pulse. This is a consequence of the assumption that the spike cut is shorter than the period T_0. Then the influence of the spike spectrum is negligible because $\tilde{f}_S(\omega) \approx \tilde{f}_S(0)$.

To complete the analysis of deterministic uncertainties, we briefly consider the case of uncertainties with alternating signs having oscillatory character, e.g., $f(t) = \mathrm{Im}[a(t)\exp(\,j\omega_f t)]$, where $a(t) > 0$ is the amplitude function. We assume that the uncertainty duration is of the order of the pulse duration, so the spectrum $\tilde{f}(\omega)$ will have a peak at $\omega = \omega_f$ and will be wider than $\tilde{\Phi}_{\mathrm{sm}}(\omega)$ and $\tilde{\Phi}_0(\omega)$. Under these conditions we may consider $\tilde{f}(\omega)$, $\tilde{S}(\omega)$, and consequently $\tilde{\mathcal{F}}(\omega)$ to be slowly varying functions of ω within the essential integration intervals around $\omega = 0$ and $\omega = \pm\omega_0$. Then, following the same procedure as in the case of a pulse cut, on the basis of Eqs. (7a)–(7c) we obtain an estimate of the retrieval error in the form

$$\delta_\Phi(z = ct/2) \approx -(\, p_{\mathrm{un}}/p_{\mathrm{eff}})\Phi_{\mathrm{sm}}(z = ct/2) - |\mathcal{F}(\omega_0)|\Phi_0[z - z_{\mathrm{sh}}(\omega_0)], \tag{10}$$

where $z_{\mathrm{sh}}(\omega) = (c/2\omega)\arg[\mathcal{F}(\omega)]$ is a spatial phase shift. Relation (10) shows that the uncertainty leads, proportionally to $p_{\mathrm{un}}/p_{\mathrm{eff}}$, to an elevation or a lowering (depending on the sign of p_{un}) of Φ_r as a whole with respect to Φ. Besides, the second term on the right-hand side of relation (10) indicates additional amplitude and phase distortions of Φ_0 (see as well the case of the pulse cut).

B. Random Uncertainties

In this subsection we consider the retrieval errors caused by random uncertainties with correlation time $\tau_c \gg \tau_{\mathrm{eff}}$, by fluctuating spike cuts, and by random uncertainties with correlation time $\tau_c \ll \tau_{\mathrm{eff}}$.

In the first case, when $\tau_c \gg \tau_{\mathrm{eff}}$, the whole measured pulse shape fluctuates from shot to shot. Then by use of Eq. (4) we estimate the corresponding rms error as

$$\sigma_\Phi(z = ct/2) = \langle|\delta_\Phi(z = ct/2)|^2\rangle^{1/2} \approx (\sigma_{p_{\mathrm{un}}}/p_{\mathrm{eff}})\overline{\Phi}(t)\,, \tag{11}$$

where $\langle p_{\mathrm{un}}\rangle = 0$ and $\langle {p_{\mathrm{un}}}^2\rangle^{1/2} = \sigma_{p_{\mathrm{un}}}$; $\langle\cdot\rangle$ denotes ensemble average. According to relation (11), an averaging of $S_m(\vartheta)$ over a number N of laser shots, before application of Eq. (2), will reduce σ_Φ $\sqrt{N}$ times because of the reduction of $\sigma_{p_{\mathrm{un}}}$ in the same proportion.

A fluctuating spike cut may arise even at a stable pulse shape with a short spike because of the fluctuations of the positions of the sampling pulses with respect to the laser pulse emission. In this case we may neglect the fluctuations of p_R and $p_R(\omega_0)$ and use relation (9) to determine the statistical retrieval error $\sigma = ({\sigma_m}^2 + {\sigma_r}^2)^{1/2}$, where $\sigma^2 = \langle{\delta_\Phi}^2\rangle$, $\sigma_m = \langle\delta_\Phi\rangle$, and $\sigma_r = \langle(\delta_\Phi - \sigma_m)^2\rangle^{1/2}$. Obviously, the expression of σ has the same form as that of relation (9), where p_S should be replaced by $\langle {p_S}^2\rangle^{1/2} = (\langle p_S\rangle^2 + Dp_S)^{1/2}$; $Dp_S = \langle(\, p_s - \langle p_S\rangle)\rangle^2$.

Let us further consider $f(\vartheta)$ as a random function with zero mean value, variance $D_f(\vartheta) = {\sigma_f}^2(\vartheta) = \langle|f(\vartheta)^2|\rangle$ (σ_f is the standard deviation), and correlation time $\tau_c \ll \tau_{\mathrm{eff}}$. A possible (statistically) quasi-stationary model of $f(\vartheta)$ is

$$f(\vartheta) = \sigma_f(\vartheta)\tilde{f}(\vartheta)\,, \tag{12}$$

where $\tilde{f}(\vartheta)$ is a statistically stationary Gaussian-distributed and Gaussian-correlated zero-mean random function with variance $D_{\tilde{f}} = 1$ and correlation time τ_c. The value of $\sigma_f(\vartheta)$ does not change essentially within time intervals of the order of τ_c. The variance D_f may be modeled as $D_f(\vartheta) = \gamma^2 S^2(\vartheta)$, where $0 < \gamma \le 1$. At a given realization of $f(\vartheta)$ the retrieval error δ_Φ is described by Eq. (3) or Eqs. (7a)–(7c). It is reasonable to assume that when $f(\vartheta)$ is many times as long as τ_c, its spectral amplitude profile $|\tilde{f}(\omega)|$ will closely follow the profile of $\langle|\tilde{f}(\omega)|^2\rangle^{1/2} \propto [I_f(\omega)]^{1/2}$, where $I_f(\omega)$ is the power spectrum of $f(\vartheta)$. Consequently, the spectral width $\Delta\omega$ of $\tilde{f}$ is of the order of that of $I_f(\omega)$, i.e., $\Delta\omega \sim {\tau_c}^{-1}$. When $\tau_c \ll T_0$, the spectral width $\Delta\omega \gg \omega_0$ and we may assume that in Eqs. (7b) and (7c), $\tilde{f}(\omega) \approx \tilde{f}(\omega_0) \approx \tilde{f}(0)$. If, in addition,

$q \ll 1$, we have $\tilde{f}(0) \ll \tilde{S}(0)$. Then in the well-known procedure of using Eqs. (7b) and (7c) we obtain that

$$\delta_\Phi(z = ct/2) \approx -(p_{\text{un}}/p_{\text{eff}})\{\Phi_{\text{sm}}(z = ct/2) + |\mathcal{F}_r(\omega_0)|\Phi_0[z - z_{\text{sh}}(\omega_0)]\}, \quad (13a)$$

where $\mathcal{F}_r(\omega) = p_{\text{eff}}/[\,p_{\text{eff}}(\omega) + p_{\text{un}}]$, $p_{\text{eff}}(\omega) = (c/2)\int_0^\infty S(t')\exp(j\omega t')\mathrm{d}t'$, and $z_{\text{sh}}(\omega) = (c/2\omega)\arg[\mathcal{F}_r(\omega)]$. One can simplify the factor $\mathcal{F}_r(\omega_0)$ by neglecting p_{un} in its denominator when $|p_{\text{un}}| \ll |p_{\text{eff}}(\omega_0)|$. If $p_{\text{un}} > |p_{\text{eff}}(\omega_0)|$, one can preliminarily average $S_m(\vartheta)$ over N laser shots to a certain extent when $|\overline{p}_{\text{un}}| \ll |p_{\text{eff}}(\omega_0)|$, where $\overline{p}_{\text{un}}$ is the area of the average uncertainty $\overline{f}(\vartheta)$. Then $\mathcal{F}_r(\omega_0) \approx p_{\text{eff}}/p_{\text{eff}}(\omega_0)$, and the rms error $\sigma = \langle|\delta_\Phi|^2\rangle^{1/2}$ is described by relation (13a), in which one should replace $-p_{\text{un}}$ with the quantity $\sigma_{p_{\text{un}}}/\sqrt{N}$. For a quasi-stationary random process $f(\vartheta)$ [Eq. (12)] the value of $\sigma_{p_{\text{un}}} = (c/2)(\tau_q\tau_c)^{1/2}$, where $\tau_c = \int_{-\infty}^{\infty} K(\tau)\mathrm{d}\tau$ is the correlation time of $f(\vartheta)$, $K(\tau) = \langle\tilde{f}(\vartheta)\tilde{f}(\vartheta + \tau)\rangle$ is the correlation coefficient of $\tilde{f}(\vartheta)$, and $\tau_q = \int_{-\infty}^{\infty}\sigma_f{}^2(\vartheta)\mathrm{d}\vartheta$. Thus we obtain that

$$\sigma = [(\tau_q\tau_c)^{1/2}/(N^{1/2}\tau_{\text{eff}})]\{\Phi_{\text{sm}}(z = ct/2) + |\mathcal{F}_r(\omega_0)|\Phi_0[z - z_{\text{sh}}(\omega_0)]\}, \quad (13b)$$

i.e., $\sigma \propto (\tau_c/N)^{1/2}$. Certainly, the general principle remains valid. That is, the retrieval error is proportional to the ratio of the uncertainty area (in a statistical sense) to the true pulse area, with additional amplitude and phase distortions of the spectrum of the inhomogeneities of $\Phi(t)$.

3. SIMULATIONS

In the simulations conducted below, we use a model of $\Phi(z)$ described earlier in Ref. 8. This model (Fig. 1) consists of a smooth component $A(t - t_0)^{-3}\exp[-G(t - t_0)]$, a high-resolution component $C\sin^2[2\pi(t - t_0)/T]$ for $t_0 \le t \le G + t_0$ at near distances, and a double-peak structure introducing discontinuities at a relatively far range, which is given by the expressions $D + d^2 - (t - t_a - dT_p)^2/T_p{}^2$ for $t_a \le t \le t_a + 2dT_p$, and $D + d^2 - (t - t_a - 3dT_p)^2/T_p{}^2$ for $t_a + 2dT_p \le t \le t_a + 4dT_p$. The parameters are specified as follows: $A = 3000\ \mu\text{s}^3$, $G = 20\ \mu\text{s}$, $C = 0.1$, $T = 5\ \mu\text{s}$, $d = 0.25$, $D = 0.03$, $t_0 = 4\ \mu\text{s}$, $t_a = 70\ \mu\text{s}$, and $T_p = 7\ \mu\text{s}$. In Fig. 1 and in the following figures the abscissa is given in samples where a sample is assumed to be equal to 15 m corresponding to 0.1 μs. The model of the pulse shape $S(\vartheta)$ (typical for CO_2 Doppler lidars) is described by the expression

$$S(\vartheta) = \vartheta[(\sqrt{2e}/\tau_1)\exp(-\vartheta^2/\tau_1{}^2) + (\chi e/\tau_2)\exp(-\vartheta/\tau_2)]/S_p, \quad (14)$$

where S_p is the peak value of the numerator. The constants τ_1, τ_2, and χ may have various values in order to produce various shapes. A pulse shape with parameters $\tau_1 = 0.1\ \mu\text{s}$, $\tau_2 = 2\ \mu\text{s}$, and $\chi = 0.2$ is shown in Fig. 1.

First, we modeled a smooth uncertainty as a parabola $f(\vartheta) = \mathcal{A}[1 - (2\vartheta - \tau_0)^2/\tau_0{}^2]$ (for $0 \le \vartheta \le \tau_0$), which is added to or subtracted from the true shape $S(\vartheta)$; $\mathcal{A}$ and τ_0 are the parameters to be adjusted. The simulations conducted show that the retrieval error is approximately equal to $-(p_{\text{un}}/p_{\text{eff}})\overline{\Phi}(t)$ [see relation (5)]. An illustration of the influence of a parabolic uncertainty with parameters $\mathcal{A} = 0.025$ and $\tau_0 = 12\ \mu\text{s}$ is given in Fig. 2(a). The pulse shape used is given in Fig. 1. The obtained error $\delta_\Phi(z)$ is compared in Fig. 2(b) with the approximate dependence [relation (5)], which turns out to describe the behavior of δ_Φ correctly. One can see that $\Phi_r(z)$ is lowered with respect

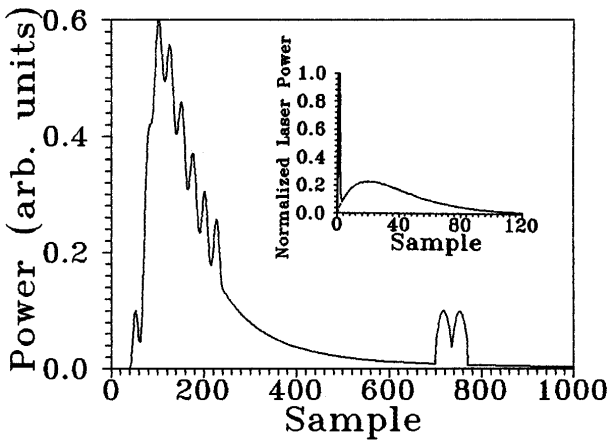

Fig. 1. Models of the original short-pulse lidar profile and (inset) of a laser pulse shape (with $\tau_1 = 0.1\ \mu\text{s}$, $\tau_2 = 2\ \mu\text{s}$, and $\chi = 0.2$) as a functions of sample number.

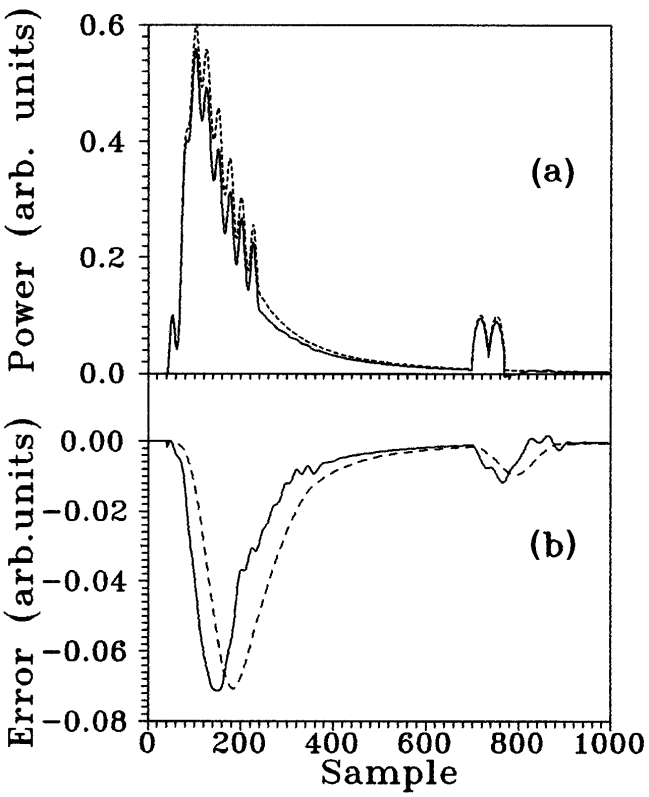

Fig. 2. (a) Original profile (dashed curve) and the profile restored by use of Fourier deconvolution (solid curve) in the case of parabolic uncertainty with $\mathcal{A} = 0.025$ and $\tau_0 = 12\ \mu\text{s}$; (b) obtained (solid curve) and estimated [Eq. (4), dashed curve] errors corresponding to the data of Fig. 2(a).

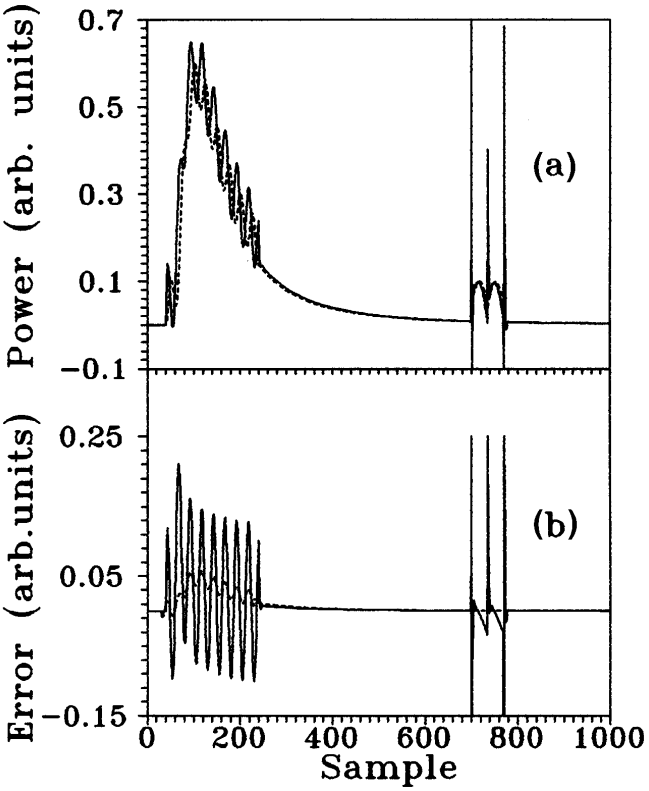

Fig. 3. Original profile (dashed curve) and the profile restored for the case of the spike cut (solid curve); (b) obtained (solid curve) and estimated [relation (9), dashed curve] errors corresponding to the data of (a).

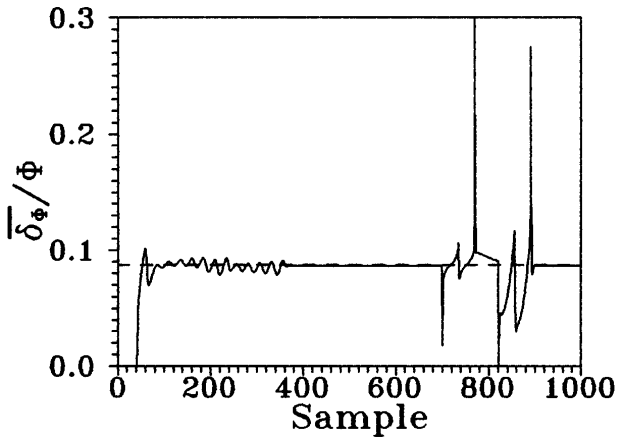

Fig. 4. Relative error $\overline{\delta_\Phi}/\Phi$ for the restored profile given in Fig. 3(a), compared with the value of p_S/p_R given by the dashed horizontal line.

to $\Phi(z)$, and there is a maximum of this lowering that is shifted with respect to the highest maximum of $\Phi(z)$ at approximately one uncertainty length in accordance with relation (5). When $f(\vartheta)$ is subtracted from $S(\vartheta)$, we obtain a similar behavior with δ_Φ, but instead of lowering we have an elevation of $\Phi_r(z)$ with respect to $\Phi(z)$.

The simulations of the effects of spike cuts confirm the theoretical conclusions [see relations (6) and (9)] about the behavior of the retrieval error δ_Φ. That is [Fig. 3(a)], the spike cut leads to an elevation of the smooth component of $\Phi(z)$ and to some increase in the amplitude and phase shift of the small-scale variations of Φ_z. One can see from Fig. 3(b) that the behavior of δ_Φ is described correctly by the approximate expression, relation (9). In Fig. 4 we compare the value of p_S/p_R with the relative error $\overline{\delta_\Phi}/\Phi$ for the restored profile given in Fig. 3(a). It can be seen that the function $\overline{\delta_\Phi}(t)/\Phi(t)$ oscillates slightly around the value p_S/p_R.

Uncertainties with alternating signs have been modeled by the expression $f(t) = qS(t)\sin(\omega_f t)$, where $0 < q < 1$. The simulations show that the restored profiles are elevated or lowered with respect to the true profile Φ when $p_{\mathrm{un}} < 0$ or $p_{\mathrm{un}} > 0$, respectively. The behavior of the obtained retrieval errors is described correctly by the approximate dependence given by relation (10). At relatively high frequencies $\omega_f \sim \omega_0$ we obtained that $|p_{\mathrm{un}}| \ll p_{\mathrm{eff}}$ and $|\tilde{f}(\omega_0)| \ll |\tilde{S}(\omega_0)|$ at values of $q \sim 0.025$. In this case the retrieval errors are small enough that there is no visible difference between the restored profile Φ_r and the original one Φ. The elevation (or the lowering) of Φ_r as well as the amplitude and the phase distortions of its small-scale structure become noticeable only at enormous values of $q \sim 0.5$.

The random uncertainties are simulated on the basis of the model discussed in Subsection 2.B [Eq. (12)] as a correlated noise with standard deviation $\sigma_f(\vartheta) = \gamma S(\vartheta)$, noise level γ, and correlation time τ_c. The results from the simulations show that the error obtained at a given realization of $f(\vartheta)$ follows closely the approximate dependence given by relation (13a). Besides, even at relatively high noise levels (e.g., $\gamma = 0.05$), the error δ_Φ is small enough that there is no visible difference between the restored profile Φ_r and the true one Φ. This is a consequence of the small values of p_{un} resulting from the small values of τ_c [see relation (13a)]. The averaging of $f(\vartheta)$ over a large number N of laser shots leads on the average to a reduction of the range of δ_Φ proportionally to $N^{-1/2}$. For instance, at an enormous noise level $\gamma = 0.5$ the visible difference between the original Φ and the restored Φ_r short-pulse profiles disappears after an averaging over 100 laser shots.

4. CONCLUSION

In the present paper we have investigated mainly the mechanism of the pulse-shape uncertainty effect on the accuracy of Fourier deconvolved lidar profiles. It is shown that the pulse-shape uncertainties of all types considered lead to an elevation or a lowering (depending on the sign of the uncertainty area) of the smooth low-frequency ($\Delta\omega_{\mathrm{sm}} \ll \Delta\omega$) components Φ_{sm} of the lidar profile. This shift up or down is proportional to Φ_{sm} and to the ratio of the uncertainty area to the true pulse area. The smooth low-frequency ($\Delta\omega \ll \tau_{\mathrm{eff}}^{-1}$) uncertainties affect the whole profile Φ in the same way. The fast-varying high-frequency ($\omega_f \gg \tau_{\mathrm{eff}}^{-1}$ or $\Delta\omega \gg \omega_0$) uncertainties lead, in addition, to amplitude and phase distortions of the small-scale high-frequency (ω_0, $\Delta\omega_0 > > \Delta\omega_{\mathrm{sm}}$) structure of the lidar profile.

In general, extremely sharp spike cuts and fast-varying alternating-sign (deterministic or random) uncertainties lead to small retrieval errors because of their small areas and small spectral amplitudes. Such uncertainties may be caused by large sampling intervals or noise. The

slowly varying prolonged uncertainties may lead to noticeable errors, but they may be avoided by suitable choice of the sampling interval. A known way to reduce the random uncertainty influence (except for spike cuts) is to average the pulse shape over a large number N of laser pulses. The simple expression derived here for this case and supported by computer simulations allows us to estimate the error and to predict the value of N that is necessary for achieving a prescribed accuracy.

The exact expression and the approximate estimates of the retrieval error δ_Φ obtained in this paper allow us, at a known order and character of the error of the pulse-shape recorder, to estimate what type of details of the lidar profile can be restored satisfactorily. In this case the error magnitude $|\delta_\Phi|$ should be much less than the amplitudes of the lidar profile components of interest, so one can determine the limitations of the Fourier deconvolution technique. On the other hand, beginning from the requirements for the quality of the lidar profile restoration, one can formulate the requirements for the accuracy of the pulse-shape recorders.

ACKNOWLEDGMENTS

The authors are grateful to one of the anonymous reviewers of Ref. 8 for directing their attention to the importance of the problem investigated in this paper. The research described in this paper was supported in part by Bulgarian National Science Foundation grant F-63.

The authors may be contacted by e-mail, ie@bgcict, or fax, 011 (359-2) 757 053.

REFERENCES

1. J. Gilbert, J. L. Lachambre, F. Rheault, and R. Fortin, "Dynamics of the CO_2 atmospheric pressure laser with transverse pulse excitation," Can. J. Phys. **50,** 2523–2535 (1972).
2. M. R. Haris and D. V. Willetts, "Performance characteristics of a TE CO_2 laser with a long excitation pulse," in *Coherent Laser Radar: Technology and Applications*, Vol. 12 of 1991 OSA Technical Digest Series (Optical Society of America, Washington, D.C., 1991), pp. 5–7.
3. R. M. Measures, *Laser Remote Sensing: Fundamentals and Applications* (Wiley, New York, 1984).
4. P. W. Baker, "Atmospheric water vapor differential absorption measurements on vertical paths with a CO_2 lidar," Appl. Opt. **22,** 2257–2264 (1983).
5. M. J. Kavaya and R. T. Menzies, "Lidar aerosol backscattering measurements: systematic, modeling, and calibration error considerations," Appl. Opt. **24,** 3444–3453 (1985).
6. Y. Zhao, T. K. Lea, and R. M. Schotland, "Correction function in the lidar equation and some techniques for incoherent CO_2 lidar data reduction," Appl. Opt. **27,** 2730–2740 (1988).
7. Y. Zhao and R. M. Hardesty, "Technique for correcting effects of long CO_2 laser pulses in aerosol-backscattered coherent lidar returns," Appl. Opt. **27,** 2719–2729 (1988).
8. L. L. Gurdev, T. N. Dreischuh, and D. V. Stoyanov, "Deconvolution techniques for improving the resolution of long-pulse lidars," J. Opt. Soc. Am. A **10,** 2296–2306 (1993).
9. L. L. Gurdev, D. V. Stoyanov, and T. N. Dreischuh, "Inverse algorithm for increasing the resolution of pulsed lidars," in *Coherent Laser Radar: Technology and Applications*, Vol. 12 of 1991 OSA Technical Digest Series (Optical Society of America, Washington, D.C., 1991), pp. 284–287.
10. T. N. Dreischuh, D. V. Stoyanov, and L. L. Gurdev, "Statistical characteristics of Fourier-deconvolved NOAA 10.6-μm ground-based lidar data," presented at the 7th Conference on Coherent Laser Radar Applications and Technology, Paris, July 19–23, 1993.
11. D. Stoyanov, L. Gurdev, T. Dreischuh, Ch. Werner, J. Streicher, S. Rahm, and G. Wildgruber, "One approach to improve the resolution of Doppler lidars," presented at the 7th Conference on Coherent Laser Radar Applications and Technology, Paris, July 19–23, 1993.
12. T. N. Dreischuh, L. L. Gurdev, and D. V. Stoyanov, "Influence of the pulse-shape uncertainty on the accuracy of the inverse techniques for improving the resolution of long-pulse lidars," in *Optics as a Key to High Technology: 16th Congress of the International Commission for Optics,* Gy. Akos, T. Lippeny, G. Lupkovics, and A. Podmaniczky, eds., Proc. Soc. Photo-Opt. Instrum. Eng. **1983,** 1060–1061 (1993).
13. Ch. Werner, G. Wildgruber, and J. Streicher, *Representativity of Wind Measurement from Space*, Final Report, European Space Agency Contract No. 8664/90/HGE-I (German Aerospace Research Establishment, Munich, 1991).